Structure, Vol. 12, 537–545, April, 2004, ©2004 Elsevier Science Ltd. All rights reserved. DOI 10.1016/j.str.2004.03.011

Automated Sample Mounting Technical Advance and Alignment System for Biological Crystallography at a Synchrotron Source

Gyorgy Snell,[1,4] Carl Cork,[1] Robert Nordmeyer,[2] Earl Cornell,[2] George Meigs,[1] Derek Yegian,[2] Joseph Jaklevic,[2] Jian Jin,[2] Raymond C. Stevens,[3] and Thomas Earnest[1,*]

[1]Berkeley Center for Structural Biology
Physical Biosciences Division
Lawrence Berkeley National Laboratory
Berkeley, Califonia 94720

[2]Engineering Division
Lawrence Berkeley National Laboratory
Berkeley, California 94720

[3]Department of Molecular Biology
The Scripps Research Institute
La Jolla, California 90237

Summary

High-throughput data collection for macromolecular crystallography requires an automated sample mounting and alignment system for cryo-protected crystals that functions reliably when integrated into protein-crystallography beamlines at synchrotrons. Rapid mounting and dismounting of the samples increases the efficiency of the crystal screening and data collection processes, where many crystals can be tested for the quality of diffraction. The sample-mounting subsystem has random access to 112 samples, stored under liquid nitrogen. Results of extensive tests regarding the performance and reliability of the system are presented. To further increase throughput, we have also developed a sample transport/storage system based on "puck-shaped" cassettes, which can hold sixteen samples each. Seven cassettes fit into a standard dry shipping Dewar. The capabilities of a robotic crystal mounting and alignment system with instrumentation control software and a relational database allows for automated screening and data collection to be developed.

Introduction

In order to realize high-throughput macromolecular crystallography, automation of the structure determination process, from target selection to structure interpretation is required (Abola et al., 2000; Rupp et al., 2002). These new developments are especially beneficial to efforts in structural genomics and rational drug design, where large numbers of structures are to be solved (Stevens et al., 2001a, 2001b). These new tools are designed to assist the non-"high-throughput" users as well by increasing the overall speed and accuracy of data collection. An automated cryogenic crystal mounting/alignment system (automounter) has been developed at Lawrence Berkeley National Laboratory which is installed on several of the protein crystallography experimental stations at the Advanced Light Source synchrotron. Systems of similar purposes for rotating anode sources have been developed at Abbott Laboratories (Muchmore, et al., 2000), as well as for experimental stations at the Stanford Synchrotron Radiation Laboratory (Cohen, et al., 2002).

There are several benefits to using an automounter system: (i) Synchrotron beam time is limited and thus should be used as efficiently as possible. (ii) Crystallography experiments are installed in radiation shielding hutches, which are inaccessible by humans during data collection. A manual sample change requires opening and closing the hutch, initiating the interlocks and performing a hutch search. This can take several minutes. (iii) An automounter can facilitate a fully automated experimental station which can be used for remote data collection and integration into a higher-level control system, where automated data processing and structure solving software can influence the data collection process (e.g., crystal ranking and data collection strategy determination). (iv) Due to the high efficiency of the system, the experimenter can evaluate a large pool of samples and select the best crystal from the set. This enables collection of higher quality data. (v) Mounting and dismounting of crystals can be done reliably reducing risk to crystals due to manual handling. (vi) Systematic studies of experimental protocols can be performed in a manner and amount that would be impractical for humans to perform. Furthermore, this can allow for an intelligent system to "learn" improved methods of data collection and processing.

The automounter system was designed to be of minimum complexity, easy to maintain, highly reliable, ideally suited for the given task, have a small footprint (since space at experimental stations is limited), and have random access to a large number of samples stored in liquid nitrogen. At the same time, technical problems related to the low temperature of the samples had to be overcome, such as keeping the sample at LN2 temperature during the whole mounting process, avoiding buildup of ice on external components, and reducing thermal expansion and conductance at LN2 interfaces. Our implementation is based to a large extent on pneumatic actuators, localized temperature controllers, and a few motorized stages which require only a relatively simple control system.

Experimental Station with Automounter

The automounter was designed for use with a variety of experimental station configurations. The only significant constraint in the use of this design is that the nitrogen cold stream subsystem must be oriented off axis from the primary goniometer axis. Almost any other configuration can be accommodated. The first automounter was installed on experimental station BL5.0.3 at the Advanced Light Source, a fixed wavelength station with significant access constraints. Shortly thereafter, systems were installed on a second monochromatic experimental station, BL5.0.1, and also on a multiwavelength

*Correspondence: tnearnest@lbl.gov
[4]Present address: Syrrx, Inc., San Diego, California 92121.

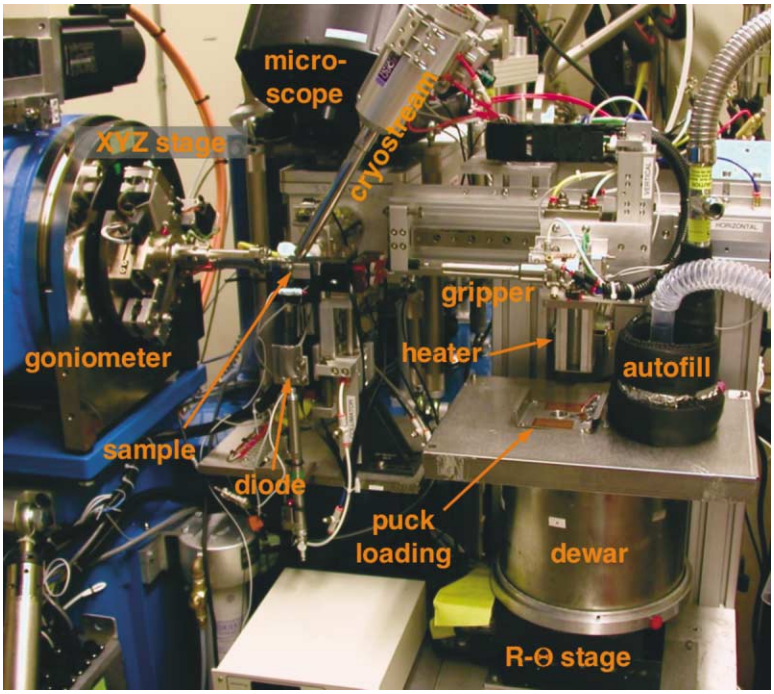

Figure 1. Overview of the ALS Experimental Station BL5.0.3 with Automounter

experimental station, BL5.0.2 (Padmore, et al., 1995; Earnest, et al., 1996). The automounter configuration is essentially identical for all three experimental stations. We are currently designing a slightly modified configuration, which will work within even more spatially constrained experimental enclosures.

Figure 1 shows an overview of the ALS experimental station BL5.0.3. The main components of the automounter setup are: a rapid sample rotation and alignment subsystem, a retractable collimator/beamstop assembly, a retractable cryostream, a long-range video microscope, and a sample mounting subsystem. Figure 2 is a close-up view of a similar system at experimental station BL5.0.2. This station has multiwavelength capability and contains an additional fluorescence monitor for the determination of anomalous absorption edges. The collimator/beamstop assembly and cryostream are retractable (Figure 2, inset) to provide access to the rotation and alignment subsystem during sample mounting/dismounting. The primary subsystems are further described below.

Sample Rotation and Alignment

A fully automated sample handling system requires a high-speed sample rotation and alignment subsystem. The crystal centering process involves the collection of a series of microscope images while rotating the sample over a wide angular range. This is followed by a sequence of adjustments to center the crystal in the input X-ray beam. Similarly, the crystal screening process involves taking a sequence of diffraction images at 90° angular separation.

The sample rotation and alignment subsystem was designed to meet the above requirements. It is based on a direct drive rotary airbearing stage (Fox Instruments [Precision Motion Distributors]) coupled with a three degrees of freedom (3DOF) sample manipulator. This system provides a highly variable rotation speed (0.01–360°/s), high angular resolution (0.00005°), and a small circle of confusion (<1 μm at sample). The 3DOF stage is mounted on the airbearing allowing for remote-controlled alignment of the sample. We have developed two types of 3DOF stages: a cartesian X-Y-Z stage (Figure 1) and a kinematic tripod stage (Figure 2). The stability and compactness of the tripod stage has made this approach our preferred design. The sample is viewed by a long distance microscope (Questar SZM100 [Company Seven]), which has variable zoom settings and can be controlled remotely (Figure 1). The sample can be both front and rear illuminated to achieve optimum image contrast.

Sample Mounting Robot

The sample mounting robot consists of three main components: the gripper, which holds the sample during transport from the Dewar to the goniometer while keeping it at low temperature (Figure 3); the X-Y-Θ stage, which performs the actual transport (Figure 1); and the Dewar stage, which supports the samples in a regular array submerged in liquid nitrogen and positions the selected sample for access by the transporter (Figure 1).

Figure 3 shows the sample gripper. Inside the gripper a conically shaped, brass split collet can be opened and closed by moving it in and out of a fixed tube using a small pneumatic actuator. During cool down of the gripper, a small vacuum pump sucks LN2 into the gripper to speed up the procedure. A sensor inside the collet is used to monitor its temperature. The inner tube is surrounded by a low thermal capacity outer shroud (very thin stainless steel tube), which provides a sheath flow of warm dry gas to reduce icing and frost formation during exposure to ambient, moisture-laden air. Addi-

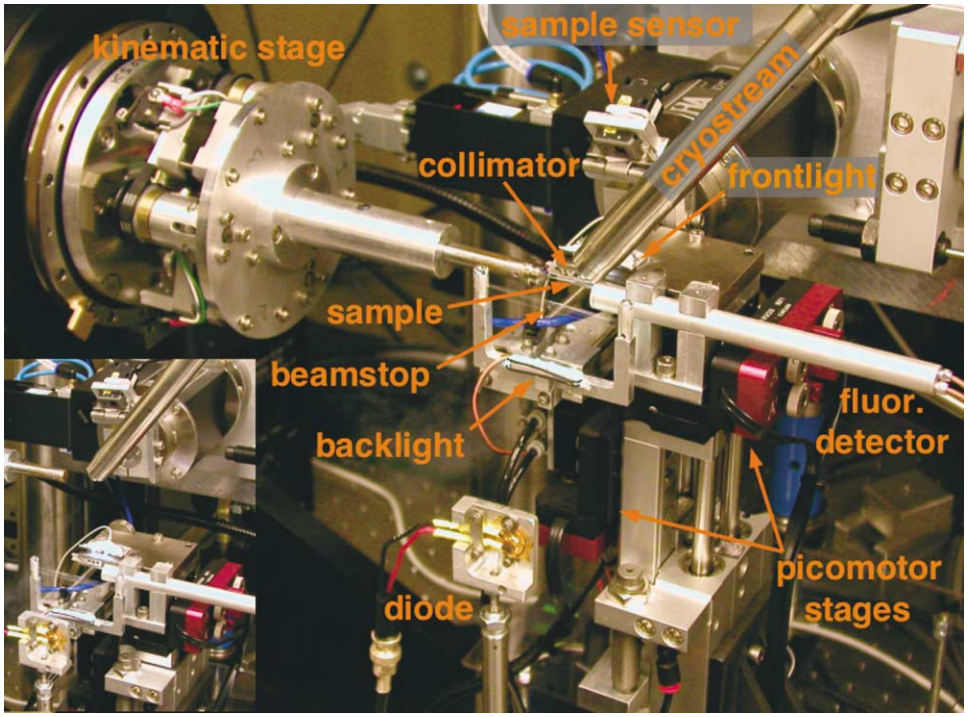

Figure 2. Close up of the ALS Experimental Station BL5.0.2 with Kinematic Stage

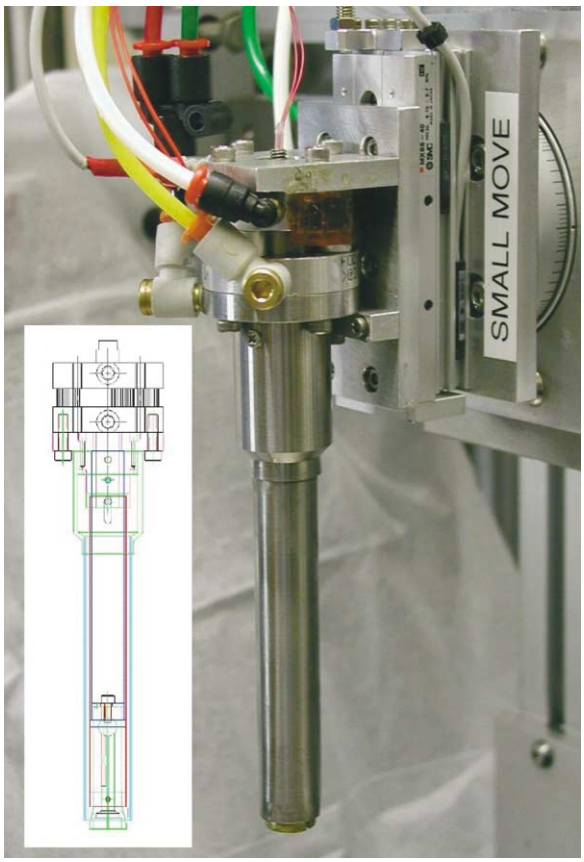

Figure 3. Sample Gripper

tionally, the gripper has a small, low-force linear stage ("small move," Figure 3). This stage is used for the final positioning of the gripper on the sample during the mounting and dismounting actions. This low-force actuator provides a more gentle handling of the crystals and also serves as equipment protection in case of a collision. The upper part of the gripper, containing the pneumatic actuator and all the connections, is equipped with a heater, to keep it warm even when the lower part of the gripper is immersed in liquid nitrogen. During continuous use, ice is periodically removed from the gripper by means of an extendable air-jet heater (Figure 1). Originally, the sample gripper was designed around the standard Hampton metal cap, which is held on the goniometer by a permanent magnet. To improve reliability of the automounter, we are using a modified cap design, which has tighter tolerances and a conical shape rather than a ledge (also available from Hampton Research as PN: HR4-779). The sample gripper is mounted on a pneumatic X-Y-Θ stage which is used to transport the samples between the goniometer and the storage Dewar. A vertical Y stage moves the gripper in and out of the Dewar, a 90° rotational Θ stage orients the gripper either horizontally or vertically, and a long horizontal X stage moves the gripper between the Dewar and the goniometer mountpoint. The pneumatic stages are all equipped with magnetic sensors, which indicate if the stage is in an extended or retracted position. These sensors not only give feedback about the state of the whole system, but they are also used to prevent collisions as part of an interlock system. Depending on the state of the automounter, certain motions are forbidden (e.g., the horizontal stage cannot be extended if the collimator is up or the gripper is in the Dewar). The

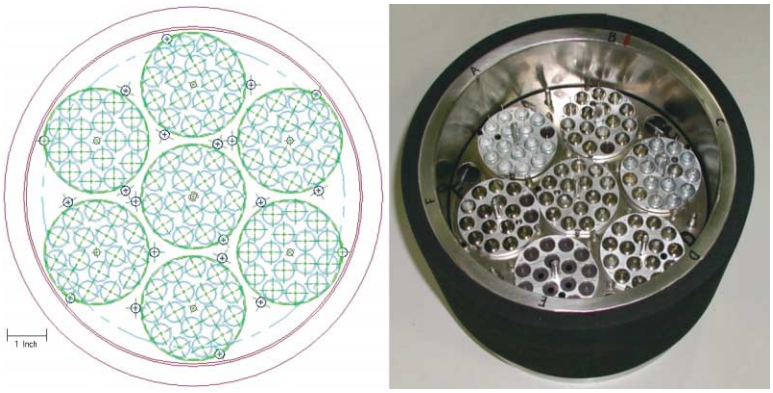

Figure 4. Liquid Nitrogen Dewar of the Automounter
Can hold a total of 112 samples (7 × 16).

motorized stages of the Dewar are also part of the interlock system.

When they are not mounted on the goniometer for data collection, the samples are maintained in a small cylindrical Dewar (see Figure 4). They are held in a custom cassette (described below), which facilitates automated handling and bulk transport. Up to seven cassettes (112 samples) can be loaded into the sample Dewar. The Dewar is mounted on an R-Θ motorized stage, which is used to position the selected sample for access by the gripper. The Dewar can also be positioned such that the gripper will be inserted into an unoccupied space during a precooling action when LN2 boiling might endanger samples. The Dewar is automatically filled directly from the facility LN2 supply system. During normal operations an insulated cover reduces icing and LN2 evaporation. The gripper reaches into the Dewar through a small heated hole in the cover. The sample cassettes are moved in or out of the Dewar through a small access port in the cover. An automated loading mechanism is being developed to facilitate this operation.

Control System

Due to the pneumatic actuators, the automounter control system is rather simple. Digital output modules control solenoid air valves, which move the stages. The position sensors are connected to digital input modules. Servomotors are used to drive the LN2 Dewar R-Θ stage. Incremental encoders and limit switches are used for position feedback and initialization of this stage. Temperature sensors and heaters are interfaced to standard industrial instrumentation controllers, which are based on 0-10VDC analog signals. All of the control system interfacing is handled using a decentralized, modular input-output system (WAGO I/O-SERIES_750), which connects directly to a private Ethernet network. Individual I/O modules can be added or subtracted as the configuration evolves. A serial, RS232, interface module is used to communicate with the Dewar stage motor/controllers (Animatics SM 2310 Series).

The different motions of the automounter can be actuated from a software interface either individually or through scripts which run a sequence of motions (so-called protocols). As an example, the *protocol* for mounting a crystal consists of the following steps:

1. Move goniometer stage to "zero" setting. The sample mounting post is positioned to the automounter's preset mount position. This setting is used for both mounting and dismounting operations in order to ensure repeatability of the sample orientation.
2. Retract collimator and cryostream. This provides clearance for the gripper access to the sample mounting post.
3. Precool gripper. Move Dewar to cooldown position and immerse gripper into LN2. Turn on vacuum pump to draw LN2 into gripper to speed cooldown. Wait until temperature reaches low setpoint (−140°C). Turn off vacuum pump.
4. Move Dewar to sample position. Gripper is partially immersed in LN2 and positioned just above sample.
5. Transfer sample to goniometer. Extend gripper to sample, grip sample, transfer sample to goniometer mount, release sample, retract gripper.
6. Extend collimator and cryostream. Restore collimator and cryostream to the normal operating configuration. Ready for crystal centering operations.
7. Park gripper. Move gripper to warming station for moisture removal. Dry for preset time interval (currently 30s). Move gripper to parking position (two optional locations: warming station or cooldown station, depending on mode of data collection).

Many of the above steps are composite operations which are, in turn, described by individual *protocols*.

The user interface for crystal centering is shown in Figure 5. The image of the crystal is shown in a window. In the case of "manual" crystal centering, the user clicks on the crystal and it is moved to the center position by the motorized 3DOF stage on the goniometer (i.e., its final position will coincide with the green cross on the image, which marks the projection onto the microscope axis of the intersection of the X-ray beam and the goniometer center of rotation). Afterwards the crystal is rotated 90° and centered again. For autocentering a protocol is run, which consecutively centers the loop at both 0° and 90°. The current autocentering protocol centers only the loop and fails under adverse illumination conditions. Further development is required before this protocol is ready for routine use. Under manual control, the goniometer can be moved to any angle, the zoom level

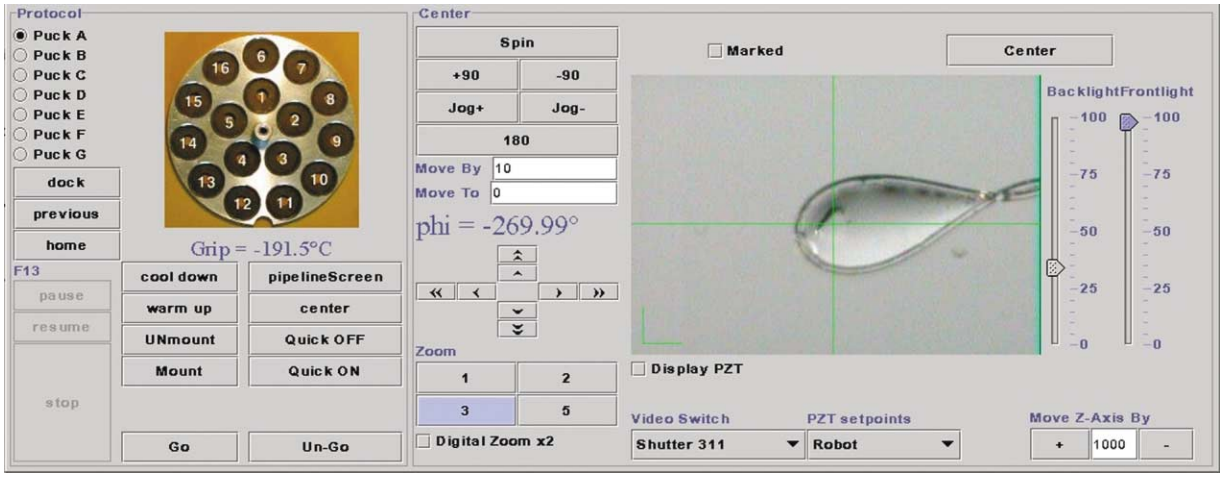

Figure 5. Part of the Graphical User Interface Used for Manual Control of the Automounter and Crystal Centering Subsystems

The area on the left is used to select samples within the Dewar and to transfer them to/from the goniometer. The area on the right is used to adjust the microscope image and to support a point-and-click centering of the crystal. See text for details.

on the microscope can be changed, the intensity of the front and rear illuminators can be adjusted, and automounter mount/dismount operations can be activated.

A database system is essential to track sample progress in any automated data collection system. For crystal tracking, we are using a relational database (MySQL Standard). Here information about the crystals, such as the puck ID and position index, the organization it belongs to, etc., is stored. The sample cassettes are labeled with barcodes (Figure 6), and they are scanned before they are put into the automounter Dewar. This system also assigns information on experimental parameters to the samples.

Sample Transport and Storage System

We have developed a sample cassette system to facilitate the rapid loading of multiple frozen samples into the automounter system (Figure 6, left). The cassette system was also designed to enable efficient, safe transport and storage of frozen samples using conventional shipping Dewars (Figure 6, right). The main considerations for the design were high sample density and compatibility with the Taylor-Wharton CP100 dry shipping Dewar.

One assembly can hold 16 samples and consists of a cassette plus a magnetic base. For transportation and storage, the cassette and base are locked together by two springs on the side of the assembly. A central post in the base is used to protect the samples and to guide the cassette during assembly. The noncircular shape of the post provides the correct orientation between the two parts. A magnetic sheet on the bottom of the base holds the samples within the base and also holds the base within the automounter (Figure 4). The cassettes are labeled with cryo-compatible barcodes for tracking.

Seven cassette assemblies can be stored in a CP100 Dewar. The pucks are placed between the shelves of a

Figure 6. Sample Cassettes and Magnetic Bases

Sample cassette holder with three cassettes ("pucks") (right). The holder fits into a Taylor-Wharton CP100 dry shipping Dewar. Magnetic bases, left.

Figure 7. Tools to Handle the Cassettes and Bases

From right to left: pusher (two pieces), base holder, straight forcep, bent forcep, cassette opener (two pieces). The forceps are used to hold the cassettes. The pusher is used to separate a cassette from the base when the samples are inserted into the automounter Dewar. The base holder is used to hold a base when it is being inserted into a cassette, usually after loading a cassette with samples. The cassette opener, inserts on the left, is used to separate the magnetic base from the cassette while keeping the samples in the latter. This can be useful for manual access to the samples.

cylindrical holder and springs hold them in place (Figure 6, right). The samples are stored upside down, so some liquid nitrogen can be preserved in the openings of the cassettes. To secure the pucks during transportation, a metal rod is inserted into the holder through all the cassette assemblies. The sample cassette system and their associated tools are shown in Figure 7 and are commercially available (Boyd Technologies).

Results and Discussion

The significance of the automation of the crystal mounting and alignment steps in the structure determination process can be seen from Table 1. During screening of crystals (e.g., taking four frames each), the time gain is a factor of 5–6. The highest resolution data so far (1.2 Å, $R_{sym} = 0.036$), using the automounter for screening and subsequent mounting of the crystal on experimental station BL5.0.3, were collected (Shouldice et al., 2003) on a bacterial iron binding protein target (periplasmic ferric ion binding protein A [PhFbpA]). To investigate the automounter's performance and reliability, and especially to find out how numerous mounting and dismounting cycles would effect diffraction quality, a PhFbpA crystal was mounted and dismounted 14 times using the automounter. A short dataset was collected (40 frames with $\Delta\varphi = 0.5^\circ$ each) after each mounting. After the fourteenth mounting, the crystal was left on the goniometer, and an additional six datasets were collected with the same settings. In addition, two large datasets (180 frames with $\Delta\varphi = 0.5^\circ$ each) were collected at the beginning and at the end of the experiment (datasets 1 and 21). All datasets were processed to 1.3 Å resolution using the HKL2000 program (10). The beam intensity was kept constant for each dataset by detuning the prefocusing mirror of the experimental station to compensate for the storage ring current decay. The beam intensity (I_0) was monitored by a photodiode downstream of the collimator (Figure 1).

Table 1. Comparison of Manual and Automated Crystal Mounting and Centering Times

Task	Manual	Automated
Load Dewar[1]		5 s
Mount crystal[2]	5 min	10 s
Center crystal	5 min	30 s
Screen crystal (4× 30s frames)	2 min	2 min
Dismount crystal	5 min	10 s
Unload Dewar[1]		5 s
Total	17 min	3 min

The times for the manual process are rough estimates and may vary largely.

[1] Loading or unloading the automounter Dewar with 112 samples (7 pucks) takes approximately 10 minutes, i.e., ~5 s/sample. This includes the hutch access and search.

[2] The crystal mounting procedure includes the positioning of the automounter Dewar (2 s), the actual mounting process of gripping the crystal, moving from the Dewar and placing on the goniometer (4 s), and the reintroduction of the gripper into the Dewar (2 s).

The statistics for the two longer datasets are given in Table 2. It can be seen, that $I/\sigma(I)$ is lower and R_{sym} is higher for the second dataset. This indicates slight radiation damage to the crystal, which is not surprising after collecting over 1,000 diffraction images. The slight increase in unit cell volume might also corroborate this observation. Optical images were taken after every mounting and after the twentieth dataset. Twelve of those images are shown in Figure 8. After the twelfth mounting, some contamination was visible on the surface of the crystal, which appeared to be ice particles at first (Figure 8). However, the corresponding diffraction image did not show any ice rings, and the data processing results also didn't indicate the presence of ice (see below).

Processing results for the 20 short datasets, together with I_0, are shown in Figure 9. The beam intensity I_0

Table 2. Data Processing Results for the First and Last Datasets

	Dataset 1	Dataset 21
Resolution (Å)	50–1.3	50–1.3
Space group	C222	C222
Unit cell dimensions (Å)	96.96/188.29/45.56	96.93/188.75/45.59
Completeness (%)	77.9 (70.2)	85.2 (78.2)
$I/\sigma(I)$	20.7 (2.0)	16.3 (1.6)
R_{sym}	0.056 (0.52)	0.056 (0.613)
Data coll. starting angle (°)	0	−8.4

Numbers in parentheses are for the highest resolution shell. The data collection starting angle change was deduced from the indexed crystal rotation around the goniometer axis (rotx in HKL2000).

was measured at the beginning and at the end of each dataset and the mean value of those two measurements is shown in the plot. It can be seen that the intensity variation between datasets was less than 5% (the horizontal line represents the mean value of I_0 of all datasets). During refinement of the diffraction data, the orientation of the crystal with respect to the laboratory system is determined. The rotation of the crystal around the goniometer spindle axis (which is horizontal in our case) is denoted by rotx, around the X-ray beam propagation direction by rotz and around the third Cartesian axis by roty (Otwinowski and Minor, 1997). Throughout the 14 mounting/dismounting cycles rotz and roty remained basically the same (the former changed by 0.3° and the latter by 0.05°). Rotation around the goniometer axis rotx, however, shows a larger deviation between cycles (see Figure 9). During the first 10 cycles, rotx changed on average +1°, in the next 2 cycles −1°, and it did not change in the last 2 cycles. The biggest single change between cycles was 2.3°. We believe that this variation is caused by the absence of indexing features on the sample base pins and also by slight systematic alignment errors in the automounter. The implication of this variation is that when the crystal is mounted anew, one has to consider a possible shift in the absolute goniometer rotation value. Starting at the same goniometer position will yield a somewhat different wedge of data. This effect was observed in our tests, the data completeness changed between the cycles as rotx was changing (Figure 9, rotx and completeness were fitted with two linear equations each). To counter this problem when predicting the data collection strategy based on screening images, we always start data collection at a 1°–2° smaller goniometer angle than given by the prediction algorithm. $I/\sigma(I)$ gradually decreases and R_{sym} increases from dataset to dataset both for the highest resolution shell and all data (Figure 9, the lines are linear fits through the data). This indicates radiation damage to the crystal is occurring. It should be especially noted, that the trend in these four parameters continues even after the fourteenth dataset, i.e., after the crystal was left on the goniometer. This shows that the changes in $I/\sigma(I)$ and R_{sym} are unrelated to the mounting/dismounting cycles. It should be noted that during standard user operation crystals are mounted mostly only twice (once for screening and once for data collection) and occasionally three times. Thus, the above results, where the crystal was cycled over 10 times without damage, confirm that the automounter is highly reliable and well suited for high-throughput structural biology, and is capable of rapid screening of crystals before full data collection is initiated.

Summary and Outlook

In summary, we have developed and built a cryogenic crystal mounting system for macromolecular crystallography, which can be used at synchrotron experimental stations. The automounter was custom built for the specific task and it is relatively simple and low-cost, has a small footprint, and is well integrated into the experimental station control system. The first automounter, installed on experimental station BL5.0.3 at the Ad-

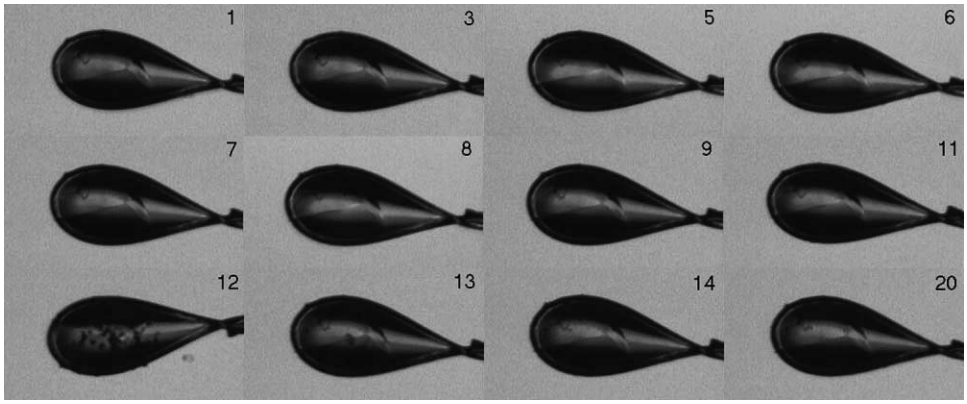

Figure 8. Images of a PhFbpA Crystal after Several Mounting and Dismounting Cycles
For details see text.

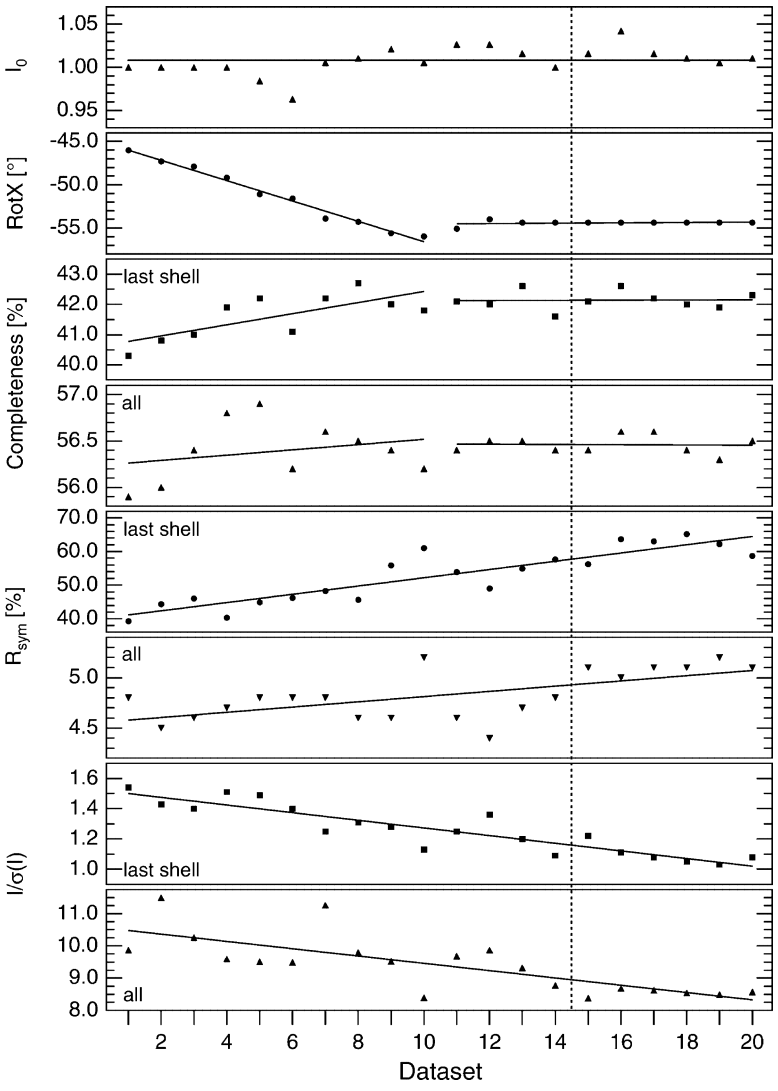

Figure 9. Results of the Data Processing for Each of the Twenty Datasets Collected

The crystal was mounted/dismounted 14 times. The last 6 datasets were collected without removing the crystal from the goniometer. Several of the parameters indicate a slow decay of the crystal due to radiation damage. See text for details.

vanced Light Source storage ring, has been in operation for over two years. The second and third stations on BL5.0.2 and BL5.0.1 have been operational for more than one year. Crystal mounting robots will soon be placed on other ALS protein crystallography experimental stations, as well as propagated to other synchrotron structural biology sites.

Several user groups currently utilize the robot on a regular basis to screen and mount crystals. Automounter users include scientists from industry (Nowakowski et al., 2002; Mol et al., 2003), academia (Shouldice et al., 2003), and structural genomics centers (Abola et al. 2000; Rupp et al., 2002). Consistent with the times listed in Table 1, screening of 16 crystals (1 cassette) with 2 × 30 s frames takes on average 35–40 min. So far, during over two years of user operation on experimental station BL 5.0.3, more than 10,000 crystals have been screened using the automounter, and several hundred datasets were collected. Due to the high reliability of the automounter, no major changes or improvements of the hardware are planned currently other than a cold-stream deflector that will allow for crystal-annealing experiments to be investigated. The high reliability allows for the automated (or semiautomated) screening of crystals to select the best crystals available for each project which should in turn improve data quality. Work remains to be done regarding software and database development to make these systems as transparent and user friendly as possible and also to further increase efficiency. Among other upgrades, improved connectivity and synchronization between the users' databases and the experimental station database is under development. Possibilities for remote experimental station/automounter operations are also being explored. For this purpose, personnel and equipment safety has to be ensured and the proper procedures have to be worked out. Furthermore, we plan to integrate the automounter system as the one step in a fully automated structure solution process utilizing smart software to control the increasingly advanced instrumentation of the experimental station and robotics in conjunction with programs which automate other steps, such as the LBNL

PHENIX project (Grosse-Kunstleve et al., 2002; Zhang et al., 2003).

Acknowledgments

We would like to thank Les Tari, Frank von Delft, Doug Dougan, Rob Skene, Cliff Mol, Jacek Nowakowski, David Hosfield, and Duncan McRee of Syrrx, and Mhairi Donohoe for their help during the commissioning of the automounter; Peter Boyd of Boyd Technologies for mechanical assistance and manufacture of the pucks and cryotools; Toni Borders, Azer Dauz, Jeff Dickert, Brian Greensmith, Anthony Rozales, and Jon Spear for support of the user and development programs; and John Taylor for control and interface software. Encouragement from Peter Schultz (Scripps/GNF) is also greatly acknowledged. This work was supported by the National Institute of General Medical Sciences of the National Institutes of Health, including funding through the Protein Structure Initiative. The Advanced Light Source is supported by the Department of Energy, Materials Sciences Division. A Web site [http://bcsb.lbl.gov/beamline/Sector5/Automounter/automounterhome.htm] features latest information and protocols.

Received: November 10, 2003
Revised: January 5, 2004
Accpted: January 7, 2004
Published: April 6, 2004

References

Abola, E., Kuhn, P., Earnest, T., and Stevens, R.C. (2000). Automation of X-ray crystallography. Nat. Struct. Biol. Struct. Genomics Suppl. *7*, 973–977.

Cohen, A.E., Ellis, P.J., Miller, M.D., Deacon, A.M., and Phizackerley, R.P. (2002). An automated system to mount cryo-cooled protein crystals on a synchrotron beamline, using compact sample cassettes and a small-scale robot. J. Appl. Crystallogr. *35*, 720–726.

Earnest, T., Padmore, H., Cork, C., Behrsing, R., and Kim, S.H. (1996). The macromolecular crystallography facility at the advanced light source biological samples. J. Cryst. Growth *168*, 248–252.

Grosse-Kunstleve, R.W., Sauter, N.K., Moriarty, N.W., and Adams, P.D. (2002). The Computational Crystallography Toolbox: crystallographic algorithms in a reusable software framework. J. Appl. Crystallogr. *35*, 126–136.

Mol, C.D., Lim, K.B., Sridhar, V., Zou, H., Chien, E.Y.T., Sang, B., Nowakowski, J., Kassel, D.B., Cronin, C.N., and McRee, D.E. (2003). Structure of a c-Kit Product complex reveals the basis for kinase transactivation. J. Biol. Chem. *278*, 31461–31464.

Muchmore, S.W., Olson, J., Jones, R., Pan, J., Blum, M., Greer, J., Merrick, S.M., Magdalinos, P., and Nienaber, V.L. (2000). Automated crystal mounting and data collection for protein crystallography. Structure *8*, R243–R246.

Nowakowski, J., Cronin, C.N., McRee, D.E., Knuth, M.W., Nelson, C.G., Pavletich, N.P., Rogers, J., Sang, B., Scheibe, D.N., Swanson, R.V., et al. (2002). Structures of the cancer-related Aurora-A, FAK, and EphA2 protein kinases from nanovolume crystallography. Structure *10*, 1659–1667.

Otwinowski, Z., and Minor, W. (1997). Processing of X-ray diffraction data collected in oscillation mode. In Methods in Enzymology, vol. 276, C.W. Carter, Jr., and R.M. Sweet, eds. (San Diego, CA: Academic Press), 307–326.

Rupp, B., Segelke, B.W., Krupka, H.I., Lekin, T.P., Schafer, J., Zemla, A., Toppani, D., Snell, G., and Earnest, T. (2002). The TB structural genomics consortium crystallization facility: toward automation from protein to electron density. Acta Crystallogr. D Biol. Crystallogr. *D58*, 1514–1518.

Shouldice, S.R., Dougan, D.R., Williams, P.A., Skene, R.J., Snell, G., Scheibe, D.N., Kirby, S., Hosfield, D.J., McRee, D.E., Schryvers, A.B., et al. (2003). Crystal structure of Pasteurella haemolytica ferric ion binding protein A reveals a novel class of bacterial iron binding proteins. J. Biol. Chem. *278*, 41093–41098.

Stevens, R.C., and Wilson, I.A. (2001a). Industrializing structural biology. Science *293*, 519–520.

Stevens, R.C., Yokoyama, S., and Wilson, I.A. (2001b). Global efforts in structural genomics. Science *294*, 89–92.

Zhang, Z., et al. Automated diffraction image analysis and spot searching for high throughput crystal screening.

Vendor Information

Animatics Corp.
3050 Tasman Drive
Santa Clara, California

Boyd Technologies
Box 95
Manchester, California

Company Seven
Astro-Optics Division
Box 2587
Montpelier, Maryland

Hampton Research Corp.
34 Journey
Aliso Viejo, California

MySQL Inc.
2510 Fairview Avenue East
Seattle, Washington

Precision Motion Distributors
7080 Donlon Way, Suite 214
Dublin, California

Taylor-Wharton-Cryogenics
PO Box 508
Theodore, Alabama

WAGO Corp
N120 W19129 Freistadt Road
P.O. Box 1015
Germantown, Wisconsin